Theoretical study of icosahedral Ni clusters within the embedded-atom method

J. M. Montejano-Carrizales
Instituto de Física, Universidad Autónoma de San Luis Potosí, 78000 San Luis Potosí, Mexico

M. P. Iñiguez, J. A. Alonso, and M. J. López
Departamento de Física Teórica, Universidad de Valladolid, 47011 Valladolid, Spain
(Received 31 October 1995; revised manuscript received 24 April 1996)

The embedded-atom method is used to study icosahedral Ni_N clusters in the size range from 13 to 147 atoms. Two mutually exclusive structures, corresponding to different ways of covering the underlying icosahedral core, are considered and the more favorable of them is determined for each cluster size. A transition from polyicosahedral to multilayered icosahedral structure is found in very good agreement with chemical probe experiments. Enhanced stability is found after the completion of certain caps (*umbrellas*) in accordance with near-threshold photoionization mass spectra and with molecular adsorption experiments. [S0163-1829(96)03532-1]

I. INTRODUCTION

During the past years experimental support has been growing for the relevance of the icosahedral symmetry in the cluster phase of the matter. Small clusters made up of a few atoms are not simple fragments of a crystalline lattice. Structural information on free clusters comes from electron diffraction,[1] chemical reactivity studies,[2,3] and from the analysis of intensity anomalies in the abundance mass spectra.[4–10] The rare gas clusters formed in supersonic vapor expansions were the first to show icosahedral symmetry.[4] Not only icosahedral clusters with complete shells were identified, but also a picture of icosahedral growth was derived for cases when the number of atoms corresponds to incomplete shells.[5] Pair potential calculations[11] have been performed to study a model of icosahedral growth for rare gas clusters in which highly symmetric atomic positions on top of an icosahedral core are progressively occupied, giving rise to multilayered Mackay icosahedral structures.[12,13]

The intensity anomalies in the mass spectra of metallic clusters are more complicated, due to the effects driven by the bonding electrons. The filling of electronic quantum levels dominates the magic numbers of various *s-p* bonded metal clusters[14,15] in the small and medium size regimes. But for large clusters, and starting from a critical size which is very dependent on the particular metal, a pattern emerges in the mass abundance, which is interpreted as reflecting the filling of geometrical (or *atomic*) shells. That critical size is around 1500 atoms for Na (Ref. 7) and much lower for alkaline-earth clusters. For the last ones, icosahedral geometries are revealed by the mass spectra of Ba clusters between 13 and 35 atoms[6] and for more than 147 atoms in the case of Mg.[8] Information about the development of the icosahedral shells was extracted in the last case, and a model of growth by formation of capping umbrellas was proposed[8] to account for the sequence of magic numbers of Mg clusters. This type of growth, although very similar to the one accepted for rare gas clusters,[5,11] is not identical and does not produce the same magic numbers. The model sucessfully explains the near-threshold photoionization experiments on Ni and Co clusters containing between 100 and 800 atoms[10] (see Sec. IV below). In those experiments, a sharp increase in the abundance is observed at some particular cluster sizes. This is interpreted as a consequence of the sharp drop of the ionization potential after an umbrella has been completed. We have studied the correspondence between the closing of shells of atoms and the drops in the ionization potential, although for a model of spherical body-centered-cubic clusters.[16] Various theoretical studies ranging from simple monovalent metal,[17,18] to noble metal, and transition metal clusters[19–23] show that, in general, icosahedral structures are very competitive and often preferred against other shapes, except for small cluster sizes. *Ab initio* molecular dynamics studies predict icosahedral growth for Li clusters with more than 25 atoms.[24]

Two different structures based on icosahedral growth can be considered. One is the usual multilayered Mackay icosahedral (MIC) filling of the space, in which the formation of successive icosahedral layers gives rise to onionlike clusters with 13, 55, 147, ... atoms. Alternatively, by occupying certain interstitial positions of the MIC lattice, polyicosahedral structures composed of interpenetrated icosahedra (TIC) can be formed. In Sec. III, the two structures, MIC and TIC will be described in more detail. In this paper, we study the competition between these two related structures for the case of nickel clusters. For this purpose, we start with Ni_{13} and add atoms one by one until we reach Ni_{147}. In the calculations we use the embedded-atom method (EAM),[25–27] which has been previously used to study structural and thermal properties of pure and mixed transition metal and noble metal clusters.[20–23,28] The EAM produces different effective interactions between two atoms when those are in different environments in the cluster, so the scheme goes beyond the simple pair potential approximations. The geometries that we assume consist of an icosahedral core with 13 or 55 atoms, upon which atoms are added in one of the two alternative ways mentioned above. For each cluster size and for each type of covering (TIC or MIC), we optimize the structure by minimizing the cluster energy with respect to the possible site occupations and allowing for a small relaxation of the

whole cluster to reach its closest local energy minimum. In this way, the energy is obtained as a function of size for the most stable atomic arrangement (within the class allowed) on top of the icosahedral core from $N=13$ to 147 atoms. The calculational method is introduced in Sec. II, and the results are presented in Sec. III. These are discussed and compared with experiment[10,29–31] in Sec. IV. A summary is given in Sec. V.

II. EMBEDDED ATOM METHOD

The EAM, which is related to the effective medium theories, replaces the N-atom problem of the cohesion energy of a metallic system by the sum of the interaction energies of each of the N atoms with a host modeling the effect of the remaining N-1 atoms on the one in question. As those approaches are based on the density functional theory,[32] the physical quantity responsible for the interactions is the electron density. Effective medium theories were first applied to problems in which the bonding effects are well localized, as for example, an interstitial impurity immersed in a metal.[33] The real system was substituted by a simpler one consisting of the impurity embedded in a homogeneous electron gas (neutralized by an uniform positive background) of density equal to the local density of the host at the position of the impurity. This approximation gave good results for the trends in impurity binding energies and chemisorption energies.

In view of the success of such a simple approach, Daw and Baskes[26] proposed to look at every atom in a metallic system as if it were an impurity in a host formed by the rest of the atoms, this theoretical tool being named the EAM. The ansatz that Daw and Baskes used for the binding energy of the whole system is

$$E_B=\sum_i F_i(\rho_i^h)+\frac{1}{2}\sum_{i\neq j}\phi_{ij}(R_{ij}), \tag{1}$$

where ρ_i^h is the effective host density in which atom i is to be embedded, F_i is the embedding energy function, and $\phi_{ij}(R_{ij})$ is a residual core-core repulsion between atoms i and j separated by a distance R_{ij}. The effective uniform density ρ_i^h interacting with atom i is approximated as a superposition of the spherically symmetric atomic density tails ρ_j^a from the other atoms at the atom-i site. Daw and Baskes[26] obtained the functions F_i and ϕ_{ij} empirically from the physical properties of the solid, although these can be also obtained from first principles.[27] Since the superposition of free atom densities in the model ignores d-d hybridization, early or late transition metals are good candidates for this method. Assuming the universality of the embedding function, that is, its independence from the particular source of the host electron density, the EAM is very appealing for using in complex situations where computational simplicity is demanded and many-body forces are required. Following the fitting scheme of Foiles, Baskes, and Daw,[25] we use the following function to describe the core-core repulsion,

$$\phi_{ij}(R)=\frac{Z_0^2(1+\beta R^\nu)^2 e^{-2\alpha R}}{R}, \tag{2}$$

where Z_0 is the number of outer electrons of the atom, and α, β, and ν are adjustable parameters. The atomic partial densities for s and d electrons are constructed from the Hartree-Fock wave functions of Clementi and Roetti[34] for the configuration $3d^8 4s^2$ of Ni. However, to form the atomic density ρ_i^a the effective number n_s of s electrons active for embedding is considered as a fitting parameter. That number was obtained by Foiles *et al.*[25] from alloy properties, since any change in n_s produces only a rescaling in the embedding function F_i for the pure metal which does not affect the total energy. In the case of nickel, $n_s=1.5166$. The elastic constants and the vacancy formation energies of the pure metal, and the heat of solution of the alloys were the properties used for the fitting of the parameters, the values of which for Ni are $Z_0=10$, $\alpha=1.8633$, $\beta=0.8957$, and $\nu=1$ [when distances are expressed in Å and energies in eV (Ref. 25)]. In addition, the binding energy given by Eq. (1) is matched to the equation of state of Rose *et al.*[35] for a broad set of values of the lattice parameter. In this way, the function $F_i(\rho)$ is obtained in numerical form. With these ingredients the calculation of the binding energy of the cluster for a given set of atomic positions is straightforward. The EAM correctly predicts that the fcc structure is energetically favored over the hcp and bcc structures in the case of nickel.[25]

Although the parameters of the EAM have been fitted to bulk properties, the method has been also applied to surfaces[26,36,37] and clusters.[20–23,28] The applicability to those situations has been questioned, because the densities sampled at the metal surface are lower than in the bulk, and improved EAM models have been proposed in which the original embedding function $F(\rho)$ is preserved for bulk densities, but its form is modified at low electron densities in order to fit also surface properties (surface energies, relaxation, and reconstruction).[38,39] To our knowledge, these models have not been tested for clusters, although it should be desirable.

The EAM model of Voter and Chen[40] also contains some different ingredients. One is that the core-core interaction has a medium-range attractive contribution (whereas in the version of Foiles *et al.*[25] it is entirely repulsive). But the most important change is that properties of the diatomic molecule were used in fitting the embedding function and the pair interaction. The fit to the diatomic molecule lowers the binding energies of small Ni clusters,[21] rendering the EAM calculations in better agreement with *ab initio* binding energies. For example, the binding energies per atom in the extreme case of Ni_2 are 2.2 eV/at. and 0.9 eV/at. for the Foiles *et al.* and Voter-Chen parametrizations, respectively. This large difference, 1.3 eV/at., is already reduced to only 0.3 eV/at. for the case of Ni_{23},[21] and will be further reduced for larger clusters. In addition, molecular dynamics simulations have been performed by Rey *et al.*[21] for Ni clusters with $N<24$. The simulations show that the main features of the icosahedral growth, like the perfect icosahedral structure of Ni_{13} or the double-icosahedron structure of Ni_{19}, are obtained with both the Foiles-Baskes-Daw and the Voter-Chen versions of the EAM. Furthermore, energy differences between isomers, which are the relevant magnitudes in our study, are very similar. For instance, a comparison between our calculations using the Foiles *et al.* model and results obtained by Jellinek[41] using the Voter-Chen model show that the energy

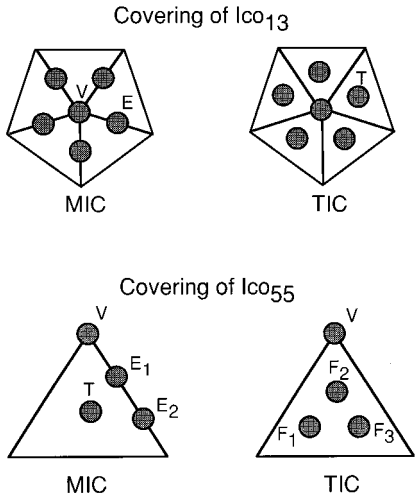

FIG. 1. MIC and TIC coverings of icosahedral clusters. Upper part: If we start with Ico_{13}, the MIC covering consists of placing atoms on top of edge (E) and vertex (V) sites. Instead, in the TIC covering, face-centered (T) and vertex (V) sites are filled. The plot shows the covering of five E (or T) and one V sites forming an umbrella. Lower part: Starting with Ico_{55}, the MIC covering fills face-centered (T), edge (E_1,E_2), and vertex (V) sites. Instead, face (F_1,F_2,F_3) and vertex (V) sites are filled in the TIC covering.

difference between the MIC and TIC isomers of Ni_{14} (see Fig. 1 for details of the two structures) is the same (0.013 eV/at.) in these two versions of the EAM. Those facts, and the good correlation with the experimental results presented in Sec. IV below, seem to indicate that the EAM, in the form parametrized by Foiles *et al.*,[25] is adequate for describing the main structural features of Ni clusters. One should be warned, however, that the specific numbers for energies should be viewed with some caution.

A lucid analysis of the EAM, and more, in general, of the *embedding* or *glue* models [26,33,42–45] has been performed by Robertson, Heine, and Payne.[46] These authors have tested a large range of *glue* models against a large database formed by 171 first-principles total energy calculations of aluminium structures with coordination number ranging from 0 to 12 and nearest neighbor distances from 2.0 to 5.7 Å. The database includes the atom, dimer, a linear chain, single layers, two-layer slabs, and three-dimensional lattices. The most important finding was that the cohesive energies are determined to a large extent by the number of nearest neighbors, a fact that is built in the formulation of the glue models. It was also concluded that the glue models for Al have a residual error which sets an upper bound on their accuracy, and warns about the reliability of those models to reproduce the small energy differences involved in structural changes. However, this conclusion applies only to the class of systems included in the database in which each system is such that all its atoms have identical environment. Robertson *et al.* expect a partial cancellation of errors in systems with many nonequivalent atoms sampling different atomic environments (such as it occurs in the simulations for clusters) and they conclude that for those systems the glue formalism may be a valid alternative to the time consuming first-principles approach.

III. RESULTS

A perfect icosahedron is formed by 20 triangular faces joined by 30 edges and 12 vertices. The smallest perfect icosahedral cluster can be labeled Ico_{13}. In this cluster one atom occupies the central position and the other 12 atoms occupy the 12 vertices of the icosahedron. We can now add atoms on top of this rigid icosahedral core in two ways. The MIC type of covering, shown in the upper part of Fig. 1, consists in adding atoms on top of edge (E) positions and vertex (V) positions. These provide a total of 30 plus 12, that is 42 sites to cover the underlying Ico_{13}, and in this way we obtain the Ico_{55}. If, instead of the edge sites, we consider sites T at the center of each triangular face (a total of 20 since there are 20 faces), then the number of covering sites is reduced to 32, and the complete covering of Ico_{13} leads in this case to a cluster with a total of 45 atoms. We name this the TIC covering. The two structures MIC and TIC are mutually excluding, so that they compete for clusters with less than 45 atoms during the process of covering the Ico_{13}. In the same way, the addition of atoms to cover Ico_{55} can be performed in the TIC mode, leading to a cluster with a total of 127 atoms. This number corresponds to the filling of the 12 vertex sites and three face sites $F_i (i=1,2,3)$ over each of the twelve triangular faces of the Ico_{55}. Alternatively, the MIC sequence could be preferred leading to a total of 147 atoms. In this case, the surface is formed by 12 vertex atoms, two atoms (E_1,E_2) on each edge (giving a total of 60 atoms) and one atom (T) at the center of each of the 20 faces. The two coverings are indicated on the lower part of Fig. 1. In the perfect MIC lattice, there are two first-neighbor distances of 1.0 and 1.05 (short bonds), in units of the radius of Ico_{13}, and a second-neighbors distance of 1.45. The distance 1.0 corresponds to first neighbors in different shells, and the distance 1.05 to first neighbors in the same shell. In the case of the perfect TIC structure, there are more bond lengths of value 1.0 than in MIC, but some of the bond lengths of magnitude 1.05 are replaced by larger ones with values 1.13 and 1.21 (the density of surface atoms of the TIC cluster is lower). The TIC pattern is favorable at the begining of a shell up to a critical size after which the MIC growth is preferred. This is understandable, because the atoms added give rise to more short bonds in the TIC mode at the first steps of covering, and in the MIC mode beyond a certain size. The crossing point depends obviously on the detailed nature of the interatomic interactions so that different systems have different crossing points.[5,24] Moreover, we show below that by allowing for a small relaxation of the rigid TIC and MIC structures the critical cluster size for which the crossing point occurs increases a little.

We now describe in detail our results for the competition between the TIC and MIC geometries for Ni_N clusters with $N=13-147$. Let us suppose for a moment that only the radius of the Ico_{13} is optimized, keeping the relations between interatomic distances fixed at their ideal values. In this case, the first five atoms added to Ico_{13} prefer the T sites over faces, that is TIC growth. However, an atomic redistribution occurs for $N=19$ that consists in the filling of five edges and their common vertex. This cap, shown in Fig. 1, forms an *umbrella* of the MIC type. There are a total of 11 bonds between the atoms forming the MIC umbrella in

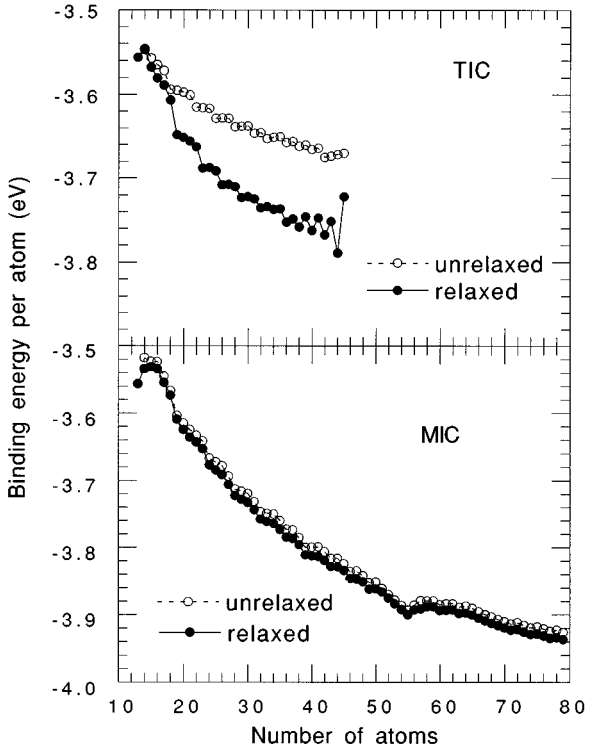

FIG. 2. Binding energy of ideal and relaxed TIC and MIC structures.

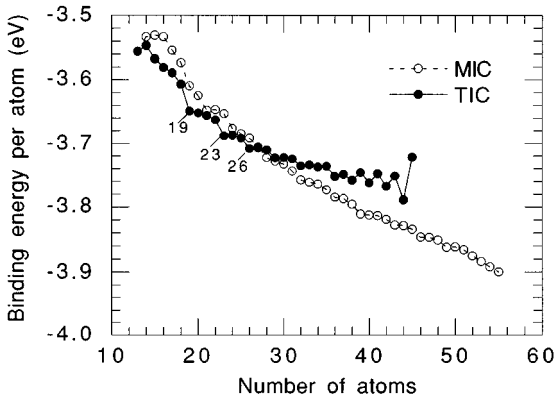

FIG. 3. Calculated binding energy per atom for Ni_N clusters with TIC and MIC structures, for $N=13-55$. Completion of TIC unbrellas at $N=19$, 23, and 26 is characterized by an enhanced stabilization.

Ni_{19} and the underlying icosahedral core, and the corresponding number of bonds for the TIC umbrella is 16, whereas the number of *intraumbrella* bonds is the same for the MIC and TIC umbrellas. Then, the preference for the MIC umbrella is motivated by the smaller bond lengths of the intraumbrella bonds, a fact that is able to balance the drawback imposed by the smaller number of bonds. When more atoms are added, MIC covering is predicted all the way up to Ico_{55}. New umbrellas grow surrounding the first one, in order to achieve the maximum number of bonds. Those umbrellas are completed at $N=19$, 24, 28, 32, 36, 39, 43, 46, 49, and 55.

However, by relaxing the ideal TIC and MIC structures up to their respective closest local energy minima in the energy hypersurface, then the TIC becomes more stable up to Ni_{27}. The relaxation is performed by the steepest-descent strategy, that is, allowing each atom, including the atoms forming the underlying icosahedral core, to move a little in the direction of the net forces acting on them. The process is repeated until the forces on all atoms vanish, and at this moment the structure of the cluster corresponds to the stable isomer nearest to the initial nonrelaxed structure. For each size and type of covering (MIC or TIC), we have relaxed different initial structures in order to find the more stable among the relaxed structures. Relaxation has a very different effect on TIC and MIC structures. Figure 2 shows that the *more open* TIC structures increase their stability substantially by relaxation, while the stability of the *more compact* MIC structures changes little. In spite of their relaxation, the TIC structures remain clearly identified and, consequently, the number of bonds coincides with the corresponding number for unrelaxed structures. Then, the relaxation of bond lengths is responsible for shifting the TIC-MIC transition from Ni_{19} to Ni_{27}. The relaxed TIC structure of Ni_{19} is a perfect double icosahedron (DIC) and can be viewed as the result of capping Ico_{13} with a TIC umbrella (see Fig. 1). The double icosahedron has two inner atoms, and relaxation reduces the interatomic distances in the capping umbrella from 1.13 and 1.21 to 1.05. The DIC was found to be the absolute energy minimum of Ni_{19} in different molecular dynamics simulations.[21,22,47–49] By adding four more atoms the next TIC umbrella is completed in Ni_{23}, the structure of which can be viewed as three interpenetrating DIC's. In the same way, an additional umbrella is completed in Ni_{26}, which can be viewed as formed by five DIC's. The size variation of the binding energy corresponding to the TIC covering is shown by the black circles in Fig. 3. The special stability of the polyicosahedra with $N=19$, 23, 26, 29, and 32 is noticeable: the absolute value of the binding energy increases sharply at those particular sizes. However, this effect becomes less pronounced as the cluster size increases. The reason is that the DIC's are not perfect for clusters other than Ni_{19}.[50] The strain accumulated by completing more and more TIC umbrellas (the last one is completed at $N=45$) makes the polyicosahedral structure eventually less stable with respect to the MIC structures, and it is responsible for the crossing between the TIC and MIC curves in Fig. 3. Ni_{26} is the largest TIC cluster that is more stable than its MIC isomer. The two structures are degenerate for Ni_{27}, and a complete reordering occurs for Ni_{28}: all the atoms on faces change to edge positions and Ni_{28} becomes a fragment of Ico_{55}. Then from this size up to Ni_{55} the cluster follows the MIC covering, and the details of this covering sequence are given in Fig. 4. Ni_{28} contains three complete MIC umbrellas, those centered on the three vertices labelled *V* in this figure. We have found that the atoms of the Ni_{28} core do not move to other sites when new atoms are added, and Fig. 4 shows the order in which the available sites are progressively filled. New MIC umbrellas are completed at $N=32$, 36, 39, 43, 46, and 49, and the cluster becomes very stable when each new umbrella becomes filled. This can be appreciated in Fig. 5, where we have plotted the difference between the total binding energies of the (more stable) N and N-1 atom clusters,

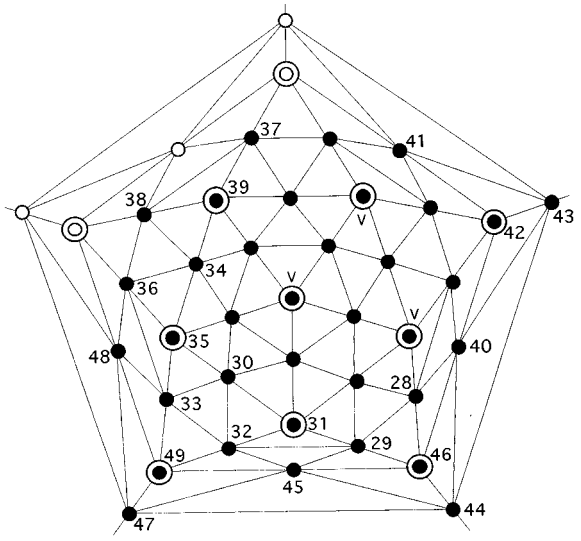

FIG. 4. The 20 faces of an unfolded icosahedron, the vertices of which are the large circles. The filled and empty small circles correspond to the occupied and empty sites in Ni_{49}, respectively. The numbers attached to some circles indicate the order in which those sites are progressively occupied during the growth of the cluster from 28 to 49 atoms. The 55th site of the icosahedron is not represented.

$$\Delta E_B = E_B(N-1) - E_B(N). \tag{3}$$

This difference gives the evaporation energy of one atom from Ni_N. Peaks appear in the evaporation energy when TIC umbrellas become completed for $N<28$, and when MIC umbrellas become completed for $N \geqslant 28$.

After nine MIC umbrellas have been completed in Ni_{49}, one vertex atom moves to an edge, and for $N=51$ all the edge sites become occupied. Then from $N=52$ to 55 the remaining vertex sites, that are nearly equivalent, are filled. This results in a nearly constant ΔE_B between $N=52$ and $N=55$. Figure 5 also shows the increase ΔN_B in the number

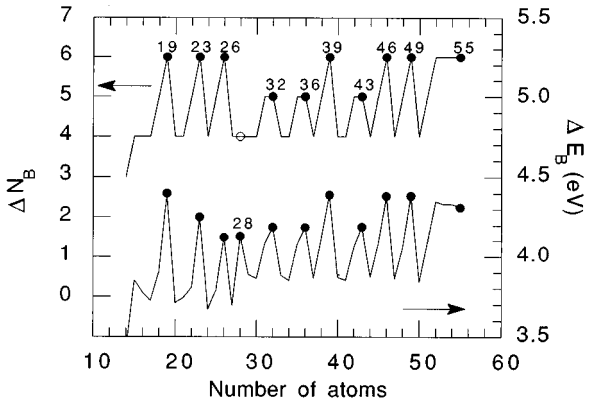

FIG. 5. Energy difference $\Delta E_B = E_B(N-1) - E_B(N)$ versus the number of atoms N in the cluster (lower curve and right-hand scale) and change ΔN_B in the number of bonds when the Nth atom is added (upper curve and left-hand scale). The numbers and black circles indicate filled umbrellas (of the TIC type for $N<28$ and of the MIC type for $N \geqslant 28$). The open circle at $N=28$ means that ΔN_B is not represented (see text).

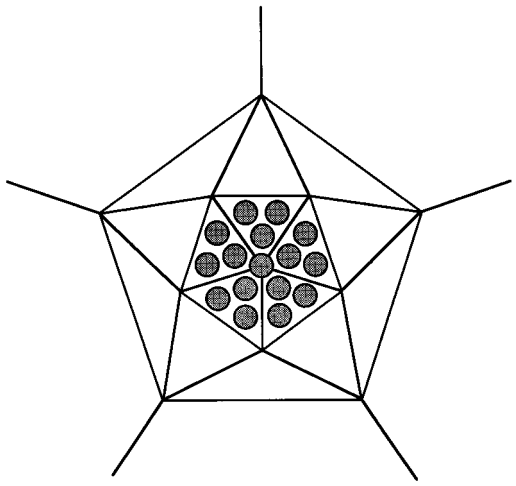

FIG. 6. Formation of a TIC umbrella in Ni_{71}.

of bonds, or equivalently in the number of first neighbors, from Ni_{N-1} to Ni_N, when atoms are progressively added to the cluster in the way just discussed. When there is no reordering of the atoms, then ΔN_B is the coordination of the last atom added, that is the minimal coordination in the cluster. ΔN_B shows a perfect correlation with ΔE_B, except at $N=28$, the size where the structural transition occurs. In fact, the TIC cluster with $N=27$ has four more bonds than the MIC cluster with $N=28$, but the bonds in the former cluster are longer and weaker than those in the later, so that Ni_{28} gains stability in spite of losing a few bonds. This kind of correlation between ΔN_B and ΔE_B does not occur for the unrelaxed structures of the TIC type. The magic numbers (or peaks in ΔE_B) predicted for the unrelaxed and relaxed TIC structures differ by one atom. This can be seen in Fig. 2, since the deviations of the binding energy curve from monotonous behaviour occur at $N=$ 18, 22, 25... for the unrelaxed TIC structures and at $N=19$, 23, 26... for the relaxed ones. This is because the last atom completing TIC umbrellas is a vertex atom which, although gaining six new bonds, five of them are of length 1.21. The relative weakness of those large bonds makes the resulting unrelaxed cluster not especially stable. Relaxation shortens those five bonds making TIC clusters with completed umbrellas very stable.

Ni_{55} is a perfect icosahedron with two shells of atoms surrounding the central atom. We now consider the formation of the third shell. The sites available for MIC and TIC coverings of Ico_{55} have been presented at the begining of this section and are shown schematically in Fig. 1. The 56th atom adopts a MIC site: a face-centred (T) site. However, after Ni_{56} the covering pattern immediately changes to TIC, and an umbrella, formed by 16 atoms, is completed at Ni_{71}. This is shown in Fig. 6. The clusters with $N=58$, 61, 64, 67, and 71 have, respectively, one, two, three, four, and five faces of this umbrella completed and the cluster with $N=74$ has one face of the next TIC umbrella completed. Filling each of those faces enhances the stability of the cluster. This can be seen in the stability function $S(N)$ defined as

$$S(N) = E_B(N-1) + E_B(N+1) - 2E_B(N) \tag{4}$$

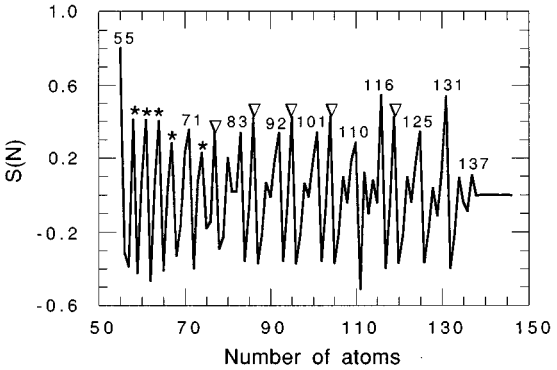

FIG. 7. Stability function $S(N)=E_B(N-1)+E_B(N+1)-2E_B(N)$. Peaks correspond to very stable clusters.

and represented in Fig. 7. This function shows peaks for particularly stable clusters. The five peaks associated with the asterisks correspond to $N=58$, 61, 64, 67, and 74. We notice that $N=71$ corresponds also to the completion of the first MIC umbrella. Figure 8 shows that the MIC and TIC structures are very close in energy for $N=72-74$, and we predict a crossing between the two structures at $N=75$. Our calculations including relaxation have been performed only up to $N=78$. For larger clusters we have assumed ideal structures, although the interatomic distance has been optimized. In addition, motivated by the transition at $N=75$, we have assumed the MIC covering from $N=79$ to $N=147$.

With a further increase of N, five more MIC umbrellas progressively develop around the first one, with closing numbers at 83, 92, 101, 110, and 116 atoms; this is schematically shown in Fig. 9. The stability function $S(N)$ of Fig. 7 shows peaks at the completion of each new umbrella. As the umbrellas develop, peaks in $S(N)$ also occur when some face sites are occupied. This occurs at $N=77$, 86, 95, 104, 119, which are labeled with triangles in the figure, and can be understood by considering the increase in the number of bonds when the cluster grows; this is shown in Fig. 10. Between $N=75$ and $N=89$ there is no redistribution of atoms when a new atom is added to the cluster, and the gain in the number of bonds is five for occupation of face sites. Three of those bonds have lengths of magnitude 1.0, whereas the lengths of the other two are 1.05. Thus, the gain in stability

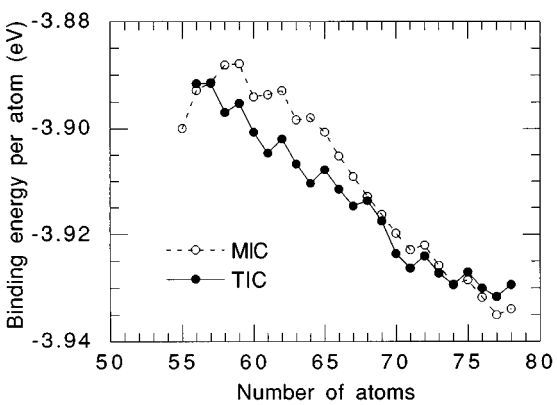

FIG. 8. Calculated binding energy per atom for Ni_N clusters with MIC and TIC structures, for $N=55-78$.

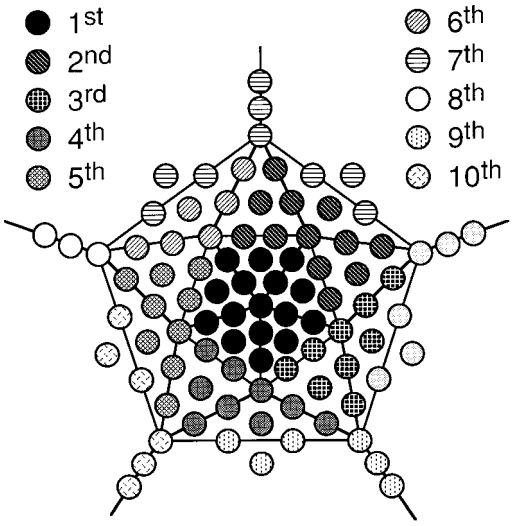

FIG. 9. Filling of the MIC lattice on top of Ico_{55}. The different symbols indicate the progressive formation of umbrellas.

results because the gain in the number of bonds of length 1.0 is maximum. For sizes larger than $N=89$, some atomic redistribution occurs as the cluster grows. First the 89th atom, which occupied the vertex position of the (incomplete) third umbrella, moves to an edge site in Ni_{90}, and the 90th atom is placed at a face site. The same reordering occurs for $N=99$ and 108 in the filling of the fourth and fifth umbrellas, respectively, and the covering sequence is similar for them. In the cluster with 110 atoms, the fifth umbrella is completed and the sixth umbrella has one vertex site, one face site, and four edge sites empty (see Fig. 9). This umbrella, which becomes completed at $N=116$, is filled in an alternating way each time a new atom is added. In the cluster with 111 atoms all the edge and face sites of the sixth umbrella become occupied at the expense of emptying the vertex sites in the other umbrellas except the first one. Similar redistributions occur in the clusters with 113 and 115 atoms. On the other hand, for the intermediate sizes $N=112$ and 114 the covering returns back to the prior sequence, that is with the first five umbrellas completed. Of course, this covering sequence neglects the effect of possible energy barriers to the motion of

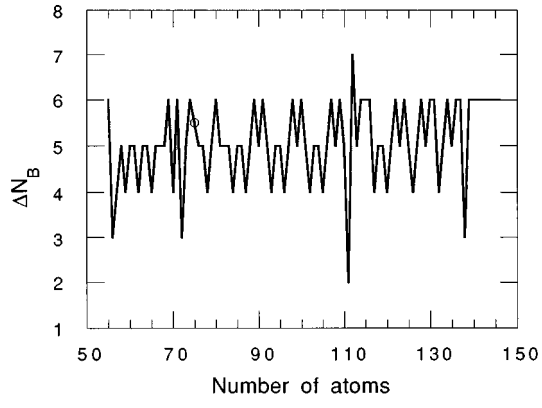

FIG. 10. Change ΔN_B in the number of bonds when the Nth atom is added for $N=55-147$. The open circle at $N=75$ means that ΔN_B is not represented.

atoms on the cluster surface. A more complete study of the growth, using molecular dynamics simulations, is required to deal with those effects. The seventh, eighth, and ninth umbrellas are filled without any disturbance of the previously existing ones, becoming completed at $N=125$, 131, and 137, respectively. The filling of the seventh umbrella follows the same pattern as the third, fourth, and fifth ones. Finally, from $N=138$ to Ico_{147} only vertex sites remain vacant, and these are filled, in close analogy to the final filling steps of the Ico_{55}.

IV. COMPARISON WITH EXPERIMENT AND WITH OTHER CALCULATIONS

The experimental mass spectra[10] of large Ni clusters containing up to 800 atoms have been explained by assuming icosahedral growth. Those results were obtained by performing near-threshold photoionization and standard time-of-flight mass spectroscopy. Strong effects were observed for $N=55$, 147, 309, and 561, which correspond to complete icosahedra. Above $N=200$, enhanced stability was observed each time a face of the icosahedron is covered, and especially when an umbrella of the MIC type is completed. In support of this view, we have obtained pronounced drops in the evaporation energy after the completion of umbrellas (see Fig. 5) and peaks in the stability function (see Fig. 7) in the range studied here, that is between 13 and 147 atoms. The clusters studied here are still small to develop the face-by-face covering of umbrellas observed in the experiments for $N>200$. However, we have found a precursor of this effect in the covering of the TIC umbrella between Ni_{55} and Ni_{71}.

Chemical probe experiments for Ni_N clusters performed by Parks and co-workers[2,29–31] point to icosahedral symmetry for $N<29$ and $N>48$. This conclusion arises from the measured saturation coverages and adsorption free energies of H_2O, NH_3, and N_2 molecules. Those measurements indicate that Ni_{13} and Ni_{55} are both perfect icosahedral clusters, and that the growth between those two sizes[31] is polyicosahedral (that is the TIC type) up to $N=26$, whereas Ni_{28} is a fragment of the Ico_{55} with three MIC umbrellas. So, the coincidence with our calculations is outstanding. We predict the transition from TIC to MIC covering at Ni_{27}. On the other hand, Parks *et al.*[31] find the structural characterization of Ni_{27} difficult. The saturation coverages are inconsistent with polyicosahedral structure and consistent with a MIC Ni_{28} cluster with an atom removed. However, the last structure would in their opinion be in contradiction with the large drop in the H_2O adsorption free energy from Ni_{27} to Ni_{28}, considering the fact that in both clusters the lowest atomic coordination would be five. The contradiction is removed within our model, by noticing the special stability of the cluster Ni_{28}. Instead of focussing on the lowest atomic coordination we look at the evaporation energy ΔE_B of Fig. 5. The peak at Ni_{28} shows that the binding between Ni atoms is especially large in this cluster and that the cluster will bind the adsorbed molecule weakly. The minimum of the experimental adsorption free energy against cluster size correlates with the calculated maximum in ΔE_B at Ni_{28}. So, in our opinion, the structure of Ni_{27} consistent with the experiments is, as Ni_{28}, a fragment of Ico_{55}. The region $28<N<48$ has not yet been studied in detail, although Parks *et al.*[31] refer to a preliminary analysis of N_2 uptake showing some evidence for fcc crystalline packing for a number of Ni clusters in this size region. However, we note a correlation between another minima in the experimental H_2O adsorption free energy at Ni_{32} and the peak in the calculated ΔE_B corresponding to the completion of four MIC umbrellas. Additional experimental work is needed to clarify matters in the region $28<N<48$. The icosahedral structure reappears clearly above Ni_{48}.[29] In addition, after completing the Ni_{55} icosahedron,[51] the experiments are consistent with TIC covering up to the completion of a 16-atom umbrella at Ni_{71}, although the structures of Ni_{66} and Ni_{67} remain unidentified yet. The binding of water molecules[3] shows minima at $N=58$, 61, and 64, for which we have found peaks in the stability function. However, there is not an experimental minimum at $N=67$, and we do not explain the minimum observed at $N=69$. There are measurements of ammonia uptake and binding of water molecules that show size oscillations correlating with the formation of MIC umbrellas for $N>71$.[3] For example, the ammonia uptake is a minimum for $N=83$, 92, 101, 116, 125, and 131, all of them having completed umbrellas. Also, the water binding is maximum for $N=72$, 93, and 102, which correspond to clusters with a single atom added to the completed umbrellas, and for $N=87$, 96, and 105; for all these clusters, we find minima in the stability function. In addition, there are maxima in water binding at $N=66$ and $N=81$ that our calculations do not explain.

Several other calculations have been performed before for Ni clusters, and Ref. 31 can be consulted for an extensive list. Molecular dynamics simulations with an *n*-body potential based on the tight-binding method were performed by Rey *et al.*[21] and by Garzón and Jellinek[47] for small clusters. Stave and De Pristo used a corrected effective medium theory,[48] and again these authors only treated small clusters ($N\leqslant 23$). EAM calculations have been performed for small,[21,22,49,52] medium,[51] and large[20,23] Ni_N clusters. All these methods give results in support of the icosahedral growth for clusters with more than 13 atoms.

Also recently, a semiempirical tight-binding scheme has been applied by Lathiotakis *et al.*[53] to compare the relative stabilities of Ni_N clusters with icosahedral structure and structures derived from the fcc (face centered cubic) lattice in the range $N=13-55$. The clusters that were actually studied were $N=13$, $N=55$, and a few selected sizes in between. The clusters were optimized at zero temperature starting from the ideal structures. The picture that comes from these tight-binding calculations is that icosahedral structures are preferred near the closed-shell sizes $N=13$ and 55, and a strong competition between the icosahedral and relaxed fcc structures is established for open-shell clusters in that size range, with some predominance of the fcc structures.

A large energy difference (0.46 eV/atom) is noticeable for $N=13$. The prediction concerning *closed-shell* clusters is consistent with our previous EAM calculations[23] comparing the relative stabilities of perfect cuboctahedral (fcc) and icosahedral closed-shell clusters with $N=13$, 55, 147, 309, 561, 923, 1415, 2057, 2869, 3871, and 5083. We have found that the icosahedral nickel clusters are more stable up to a size $N=1415$, which corresponds to seven full layers around the central atom. For larger sizes, the cuboctahedral clusters

become more stable. In the cases with an incomplete second shell, studied by Lathiotakis, the relaxed fcc structure was predicted to be more stable, although the total binding energies per atom differ less than for Ni_{13}: the differences are 0.08, 0.07, 0.05, and 0.017 eV/atom for $N=19$, 23, 24, and 38, respectively. A few more cluster sizes were considered by Lathiotakis *et al.*, but only one of the two structures was studied in each case. We recall that the reactivity experiments support the double icosahedron for Ni_{19} and the triple icosahedron for Ni_{23}. So, the tight-binding results seem to be in conflict with other calculations and with the interpretation of the chemical probe experiments,[31] except perhaps in the range $N=28-48$, where experimental information is not yet available.

We have also performed several selected calculations for clusters with a fcc structure, allowing for relaxation: cuboctahedral shapes were considered for Ni_{13} and Ni_{55}, and clusters with closed coordination shells around a central atom have been modeled representing Ni_{19} and Ni_{43} (two and three coordination shells, respectively). The EAM predicts the following energy differences between the relaxed fcc and icosahedral structures, favoring icosahedral packing: 0.081 (Ni_{13}), 0.055 (Ni_{19}), 0.074 (Ni_{43}), and 0.048 eV/atom (Ni_{55}). For Ni_{13}, the result agrees well with other calculations: a Finnis-Sinclair many-body potential[44] predicts an energy difference of 0.052 eV/at.,[54] corrected effective medium calculations give 0.089 eV/at.,[48] and *ab initio* density functional calculations give 0.095 eV/at.[55] The agreement gives confidence on the predictions of the EAM. All these values are substantially lower than the binding energy difference predicted by the tight-binding method of Lathiotakis *et al.* (0.46 eV/at.).

V. SUMMARY

Using the embedded-atom method (EAM) in the version of Foiles *et al.* [25] we have compared two types of icosahedral growth found previously to be relevant for inert gas[11] and alkaline-earth clusters.[8] Our calculations specifically refer to nickel and we have studied the covering of icosahedral Ni_{13} and Ni_{55}. First the cluster covering develops in the TIC mode, but a transition to the MIC (multilayered Mackay icosahedron) mode is predicted at $N=28$. When Ni_{55} is being covered, the TIC pattern is the preferred one up to the completion of an umbrella at $N=71$ and then changes to a MIC covering. These results are in good agreement with the chemical probe experiments (using N_2). Drastic changes in the cluster stability occur when capping umbrellas are completed and this prediction agrees with the results of near-threshold photoionization experiments for large clusters.[10] The magic character of the Ni_n clusters with completed umbrellas is also evident in measurements of the adsorption energy of ammonia and water molecules. Molecular dynamics simulations of medium size clusters[51] and a study of the energy barriers between competing icosahedral and crystalline or other structures would be desirable in order to get a full picture of cluster growth in the small and medium size range. Also, one has to notice that the structures determined from chemical probe studies are those of the clusters with the adsorbates present. In this respect, it would be interesting to perform calculations for clusters with adsorbed molecules, because adsorption could induce some structural changes in order to increase the binding between the molecule and the cluster. This is not the case for N_2 molecules, which leave completely unaltered the structure of the pure Ni clusters. On the other hand, the analysis of the experiments is based on adsorption energy data taken from surface studies; these energies could change a little in the clusters. Although distinct versions of the EAM may differ in the absolute values of the binding energies, the relative energies of *equal-size* isomers seem to be very similar. This fact supports the applicability of the EAM method for the purpose of this work.

ACKNOWLEDGMENTS

This work has been supported by DGICYT (Grant No. PB92-0645-C03-01), Junta de Castilla y León (Grant No. VA58/93), and CONACYT (Grant No. 4920-E9406). J.M.M.C. acknowledges support from MEC (Spain) during their postdoctoral stay at the University of Valladolid. J.A.A. acknowledges the hospitality and support from Queen's University (Department of Physics) during July-August 1995.

[1] J. Farges, M.F. de Feraudy, B. Raoult, and G. Torchet, J. Chem. Phys. **78**, 5067 (1983).
[2] T.D. Klots, B.J. Winter, E.K. Parks, and S.J. Riley, J. Chem. Phys. **92**, 2110 (1990); **95**, 8919 (1991).
[3] E.K. Parks, B.J. Winter, T.D. Klots, and S.J. Riley, J. Chem. Phys. **94**, 1882 (1991).
[4] O. Echt, K. Sattler, and E. Recknagel, Phys. Rev. Lett. **47**, 1121 (1981).
[5] I.A. Harris, R.S. Kidwell, and J.A. Northby, Phys. Rev. Lett. **53**, 2390 (1984).
[6] T.P. Martin and T. Bergman, J. Chem. Phys **90**, 6664 (1989); D. Rayane, P. Melinon, B. Cabaud, A. Hoareau, B. Tribollet, and M. Broyer, Phys. Rev. A **39**, 6059 (1989).
[7] T.P. Martin, T. Bergman, H. Göhlich, and T. Lange, Z. Phys. D **19**, 25 (1991).
[8] T.P. Martin, T. Bergman, H. Göhlich, and T. Lange, Chem. Phys. Lett. **176**, 343 (1991).
[9] M. Pellarin, B. Baguenard, M. Broyer, J. Lermé, J.L. Vialle, and A. Perez, J. Chem. Phys. **98**, 944 (1993).
[10] M. Pellarin, B. Baguenard, J.L. Vialle, J. Lermé, M. Broyer, J. Miller, and A. Perez, Chem. Phys. Lett. **217**, 349 (1994).
[11] J.A. Northby, J. Chem. Phys. **87**, 6166 (1987).
[12] A.L. Mackay, Acta Crystallogr. **15**, 916 (1962).
[13] J.M. Montejano-Carrizales and J.L. Morán-López, Nanostruct. Mater. **1**, 397 (1992).
[14] W.A. de Heer, W.D. Knight, M.Y. Chou, and M.L. Cohen, *Solid State Physics: Advances in Research and Applications*, edited by H. Ehrenreich, F. Seitz, and D. Turnbull (Academic Press, New York, 1987), Vol. 23, p. 1.
[15] M.P. Iñiguez, M.J. López, J.A. Alonso, and J.M. Soler, Z. Phys. D **11**, 163 (1989).
[16] J.M. Montejano-Carrizales, M.P. Iñiguez, and J.A. Alonso, Solid State Commun. **94**, 799 (1995).

[17] J. Mansikka-aho, M. Manninen, and E. Hammarén, Z. Phys. D **21**, 271 (1991).
[18] Q. Wang, M.D. Glossman, M.P. Iñiguez, and J.A. Alonso, Philos. Mag. B **69**, 1045 (1994).
[19] S. Valkealahti and M. Manninen, Phys. Rev. B **45**, 9459 (1992); Comput. Matter. Sci. **1**, 123 (1993).
[20] C.L. Cleveland and U. Landman, J. Chem. Phys. **94**, 7376 (1991).
[21] C. Rey, L.J. Gallego, J. García-Rodeja, J.A. Alonso, and M.P. Iñiguez, Phys. Rev. B **48**, 8253 (1993).
[22] J. García-Rodeja, C. Rey, L.J. Gallego, and J.A. Alonso, Phys. Rev. B **49**, 8495 (1994).
[23] J.M. Montejano-Carrizales, M.P. Iñiguez, and J.A. Alonso, J. Cluster Sci. **5**, 287 (1994).
[24] M.W. Sung, R. Kawai, and J.H. Weare, Phys. Rev. Lett. **73**, 3552 (1994).
[25] S.M. Foiles, M.I. Baskes, and M.S. Daw, Phys. Rev. B **33**, 7983 (1986).
[26] M.S. Daw and M.I. Baskes, Phys. Rev. B **29**, 6443 (1984).
[27] M.S. Daw, Phys. Rev. B **39**, 7441 (1989).
[28] J.M. Montejano-Carrizales, M.P. Iñiguez, and J.A. Alonso, Phys. Rev. B **49**, 16 649 (1994).
[29] E.K. Parks and S.J. Riley, Z. Phys. D **33**, 59 (1995).
[30] E.K. Parks, B.J. Winter, T.D. Klots, and S.J. Riley, J. Chem. Phys. **96**, 8267 (1992).
[31] E.K. Parks, L. Zhu. J. Ho, and S.J. Riley, J. Chem. Phys. **100**, 7206 (1994); **102**, 7377 (1995).
[32] P. Hohenberg and W. Kohn, Phys Rev. **136**, B864 (1964).
[33] M.J. Stott and E. Zaremba, Phys. Rev. B **22**, 1564 (1980).
[34] E. Clementi and C. Roetti, At. Data Nucl. Data Tables **14**, 177 (1974).
[35] J.H. Rose, J.R. Smith, F. Guinea, and J. Ferrante, Phys. Rev. B **29**, 2963 (1985).
[36] S.M. Foiles, Phys. Rev. **22**, 7685 (1985).
[37] M.S. Daw, Surf. Sci. Lett. **166**, L161 (1986).
[38] M.I. Haftel, Phys. Rev. B **48**, 2611 (1993).
[39] M.I. Baskes and R.A. Johnson, Modelling Simul. Mater. Sci. Eng. **2**, 147 (1994).
[40] A.F. Voter and S.P. Chen, in *Characterization of Defects in Materials*, edited by R.W. Siegal, J.R. Weertman, and R. Sinclair, MRS Symposia Proceedings No. 82 (Materials Research Society, Pittsburgh, 1987), p. 175.
[41] J. Jellinek, in *Metal-Ligand Interactions*, edited by N. Russo and D. Salahub (Kluwer Academic, Dordrecht, 1996), p. 325.
[42] F. Ercolessi, M. Parrinello, and E. Tosati, Philos. Mag. A **58**, 213 (1988).
[43] K.W. Jacobsen, J.K. Norskov, and M.J. Puska, Phys. Rev. B **35**, 7423 (1987).
[44] M.W. Finnis and J.E. Sinclair, Philos. Mag. A **50**, 45 (1984); **53**, 161 (1986).
[45] D.G. Pettifor, Phys. Rev. Lett. **63**, 2480 (1989).
[46] I.J. Robertson, V. Heine, and M.C. Payne, Phys. Rev. Lett. **70**, 1944 (1993).
[47] I.L. Garzón and J. Jellinek, in *Physics and Chemistry of Finite Systems: From Clusters to Crystals*, edited by P. Jena, S.N. Khanna, and B.K. Rao (Kluwer Academic, Dordrecht, 1992), Vol. I, p. 405.
[48] M.S. Stave and A.E. DePristo, J. Chem. Phys. **97**, 3386 (1992); M.S. Stave, D.E. Sanders, T.J. Raeker, and A.E. De Pristo, *ibid.* **93**, 4413 (1990).
[49] Z.B. Güvenç, J. Jellinek, and A.F. Voter, in *Physics and Chemistry of Finite Systems: From Clusters to Crystals*, edited by P. Jena, S.N. Khanna, and B.K. Rao (Kluwer Academic, Dordrecht, 1992), Vol. I, p. 411.
[50] J. Farges, M.F. de Feraudy, B. Raoult, and G. Torchet, Surf. Sci. **156**, 370 (1985).
[51] C. Rey, J. García-Rodeja, and L.J. Gallego, Phys. Rev. B (to be published), have shown that the icosahedron is the lowest energy structure of Ni_{55} in a molecular dynamics simulation using the Voter-Chen version of the EAM.
[52] J. Jellinek and Z.B. Güvenç, in *The Synergy between Dynamics and Reactivity at Clusters and Surfaces*, edited by L.J. Farrugia (Kluwer, Dordrecht, 1995), p. 217.
[53] N.N. Lathiotakis, A.N. Andriotis, M. Menon, and J. Connolly, Europhys. Lett. **29**, 135 (1995); J. Chem. Phys. **104**, 992 (1996).
[54] J. Uppenbrink and J. Wales, J. Chem. Phys. **96**, 8520 (1992).
[55] F.A. Reuse, S.N. Khanna, and S. Bernel, Phys. Rev. B **52**, R11 650 (1995).